

# Fluid Devices by the Use of Electrohydrodynamic Effects of Water

H. Sugiyama<sup>1</sup>, H. Ogura<sup>2</sup> and Y. Otsubo<sup>2</sup>

<sup>1</sup> *Division of Diversity and Fractal Science, Graduate School of Science and Technology, Chiba University, Yayoi-cho 1-33, Inage-ku, Chiba-shi, Chiba, 263-8522 Japan*

<sup>2</sup> *Department of Urban Environment Systems, Graduate School of Engineering, Chiba University, Yayoi-cho 1-33, Inage-ku, Chiba-shi, 263-8522, Japan*

*Email: yas.otsubo@faculty.chiba-u.jp*

## ABSTRACT

When the high DC electric fields are applied to distilled water through needle electrodes, the jet flow with velocities up to  $0.3 \text{ ms}^{-1}$  is generated in bulk from the negative to positive electrodes. The flow direction and velocity can be modified by the design of electrodes and their arrangements. By controlling the flow patterns, new types of inkjet devices and liquid motor are developed. In inkjet devices, a set of electrodes consisting of short tube and needle is vertically placed in plastic tube and the distilled water so filled in the reservoir that the electrodes are completely immersed. The application of high voltages causes the vertical flow to produce a water column with free surface. The motor consists of vane wheel, cup, two sets of electrodes, and working fluid. For aqueous solutions of ethanol and glycerin, the angular velocity of motor is measured as a function of viscosity and conductivity. The high performance of motor is achieved by the solutions with viscosity of  $0.85 \sim 1.7 \text{ mPa}\cdot\text{s}$  and conductivity of  $20 \sim 30 \text{ }\mu\text{Sm}^{-1}$ . The EHD water jets have great potential in application to new fluid devices.

**Keywords:** Electrohydrodynamic (EHD) effects, Liquid motors, Inkjet devices, Water.

## NOMENCLATURE

$D$	diameter, m	$Q$	flow rate, $\text{m}^3\text{s}^{-1}$
$E$	electric field intensity, $\text{Vm}^{-1}$	$V$	voltage, V
$F$	force, N	$\nu$	angular velocity, $\text{s}^{-1}$
$H$	height, m	$\eta$	viscosity, $\text{Pa}\cdot\text{s}$
$I$	electric current, A	$\eta_e$	electric consumption efficiency
$P$	power consumption, W	$\rho$	density, $\text{kgm}^{-3}$
$p$	pressure, Pa	$\sigma$	conductivity, $\text{S m}^{-1}$

## 1. INTRODUCTION

When a dielectric fluid is subjected to a high electric field, macroscopic motions such as convection, turbulence, and chaos are induced between electrodes. The secondary motions of fluid, which are produced in high electric fields, are known as electrohydrodynamic (EHD) effects (Castellanos, 1991; Maekawa et al., 1992; Suzuki, 1985; Worraker and Richardson, 1981). Recently the application of EHD flow to mechanical devices has received increasing attention. Zahn and Reddy (2006) have analyzed the micromixing process due to EHD

instability for techniques of separation of DNA from other cellular components. For electronic cooling, the EHD micropumps have been extensively studied by Darabi et al. (2001, 2002, 2005, 2006). In the field of colloid science, the EHD flow of suspensions, which contain nanoparticles, has been accepted as the key technology of direct writing of nanoparticles for nanoprinting and formation nanostructures (Rocks et al, 2007; Wang et al., 2007). Also, the EHD flow can be used for formation of fine fibers and this method is called electrospinning (Skotak and Larsen 2006; Park et al. 2008). According to the numerical simulation

and EHD experiments in DC fields, the velocity of the flow has been reported to be of the order of  $10^{-2}$   $\text{ms}^{-1}$  in electric fields of several  $\text{kVmm}^{-1}$  (Gosse 1988; Yasufuku et al. 1979; Haga et al. 1995). In previous papers, we have found that on the application of high DC fields to some insulating fluids, a fluid jet with a velocity of about  $1 \text{ ms}^{-1}$  is generated from the positive electrode. Because the EHD jet is very useful in applications to mechanical elements, three kinds of new fluid devices, that is, dielectric fluid motors (Otsubo and Edamura 1997; Yokota et al. 2001a, b), electrorheological devices (Otsubo and Edamura 1998, 1999), and inkjet nozzles (Edamura and Otsubo 2004) have been developed by controlling the velocity and direction of jet. The dielectric fluid motors consist of vane wheel, cup, wire electrodes, and working fluid. Several sets of wire electrodes are arranged around the inner wall of cylinder. The rotational direction is regulated by the polarity because the flow is induced in the direction from the positive to negative electrodes. The electrorheological effect is defined as a rapid and reversible change in viscosity of fluids on the application or removal of electric fields. Subjected to high electric fields in electrodes with flocked fabrics, the insulating oils can cause the increase in viscosity. The rapid and large-scale convection is generated between the tips of fibers and plate electrode. The interactions between EHD convection and external shear give rise to the additional energy dissipation and in turn the increase in viscosity. The electric fields can cause not only the body forces in the bulk, but also the extra stresses across the interfaces. In nonuniform fields generated by a needle electrode, the continuous evolution of free surface can take place from the nozzle exit. This can provide the new basic technology for inkjet printing systems.

The EHD effects are extensively studied from theoretical and experimental points. The most important agreement is that the striking EHD effects are induced for insulating oils with very low conductivity ( $<10^{-8} \text{ Sm}^{-1}$ ). Although the mechanism of jet flow is not clearly explained, the velocity and scale of EHD convection are strongly enhanced in nonuniform field conditions. The liquids with higher conductivity can be expected to show EHD effects by modification of geometry and electrode design. Therefore, the attention is focused on the water and aqueous solutions. In the present paper, the feasibility of EHD devices utilizing water and aqueous solutions as working fluids will be discussed in relation to the fluid properties.

## 2. EHD PUMP AND INKJET DEVICE FOR WATER

The working fluids were three kinds of water. The running water was underground-water in Nishi-Chiba Campus of Chiba University. The ion-exchanged water and distilled water, which were obtained by the use of Auto Still WG222 (Yamato

Science Co., Ltd), were also used. Figure 1 shows the electric conductivity plotted against the field strength. The temperature was  $25^\circ\text{C}$  for all measurements. The measurements were carried out in a parallel plate geometry, in which the sample fluids were sandwiched between the electrodes, made of stainless steel with smooth surfaces. Because of high conductivity, the accurate values were not determined for running water in high electric fields. The conductivity of ion-exchanged water and distilled water slightly decreases with increasing field intensity.

Figure 2 shows an experimental setup of EHD pump for measurements of surface elevation of liquid in electric fields. Two electrodes are placed in silicone tube. The inside diameter  $D$  is 4.0 mm. The upper electrode is a short tube made of tinned copper. The inside diameter is 2.4 mm, outside diameter is 4.0 mm, and length is 8.0 mm. The lower one is a

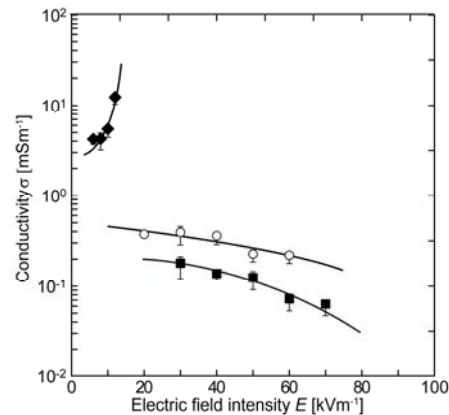


**Fig. 1. Field intensity dependence of conductivity for distilled water ( $\circ$ ), ion-exchanged water ( $\blacksquare$ ), and running water ( $\blacklozenge$ ).**

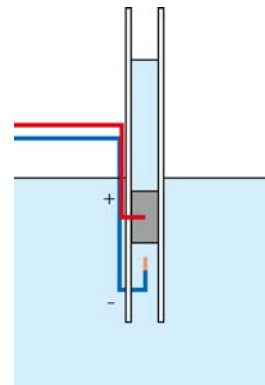


**Fig. 2. An experimental setup of EHD pump for measurements of surface elevation of liquid in electric fields.**

copper needle with a diameter of 0.12 mm. The length of tip, which is exposed to working fluids, is 1.0 mm and other part of lower electrode is covered with an insulating plastic. The tube and needle electrodes are arranged at a distance of 3.0 mm. The working fluids are so filled in the reservoir that the upper level of tube electrode is completely immersed. A DC voltage is applied to the tube electrode from a power supply manufactured by Glassman High Voltage, Inc. The voltage is in the range of 1.0 to 10 kV. The needle electrode is connected to the ground (0 V). Since the fluid level in silicone tube was instantaneously increased on the application of electric fields, the height was measured as a function of voltage.

Figure 3 shows the surface elevation  $H$  plotted against the applied voltage for distilled and ion-exchanged water. The measurements are repeated four times and error bars indicate the range of obtained data. Because of high conductivity, it was difficult to apply the voltage beyond 0.20 kV and hence significant elevation of surface was not observed for

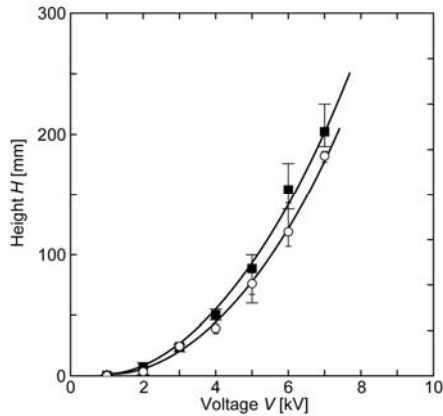


**Fig. 3. Surface elevation plotted against the applied voltage for distilled(○) and ion-exchanged water(■).**

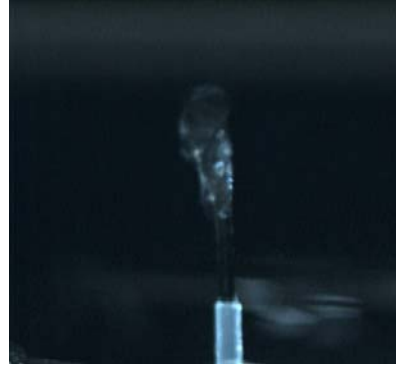


**Fig. 4. A photograph of inkjet nozzle.**

running water. On the other hand, the surface level of distilled water and ion-exchanged water remarkably increases with increasing the voltage. From the curve fitting, the quadratic effect of electric field on the surface elevation can be seen for the water with low conductivity. The current of ion-exchanged water was about 0.6 mA at 7.0 kV. But, once the highest level is achieved at a fixed voltage within a second, the surface gradually descends and the current is increased in several minutes. When the current exceeds 3mA during the process, the streamer corona was caused by the insulation destruction and the surface starts to violently move up and down. As a simplified approach, the force  $F$  induced in a tube can be estimated by the following equation,

$$F = \rho(\pi D^2/4)Hg = (\pi D^2/4)p \quad (1)$$

where  $\rho$  is the density of water,  $D$  is the diameter of the tube,  $H$  is the surface elevation,  $g$  is the gravitational acceleration, and  $p$  is the pressure in water column. It can be estimated that the induced force and pressure are about  $2.2 \times 10^{-2}$  N and  $1.7 \times 10^3$  Pa, respectively, at 7.0 kV for ion-exchanged water. Bologa and Kozhevnikov (2008) have developed the EHD pumps consisting of plate with holes and wire electrode and shown the quasi-quadratic dependence of pressure on the effect of electric field. The induced pressures are reported to be of the order of  $10^3$  Pa in the range of 10–20 kV depending on the electrode arrangement. Although the working fluid is kerosene in their study, it must be stressed that the similar EHD behavior is observed for water in the present work.

Instead of long silicone tube, a short plastic nozzle with the diameter of 2mm was set just above the tube electrode. This provides a prototype of inkjet devices. The application of high voltages causes the vertical flow to produce a water column with free surface, a typical picture of which is shown in Fig. 4. The height of water column and the flow rate were measured at different voltages. Figure 5 shows the results for ion-exchanged water. The flow issues when the voltage is increased above a certain level. Because of difference in diameters, the backward flows occur in the space between tube electrode and of nozzle tip at low voltages. The ejection of water from the nozzle may be

suppressed by the backward vortex flows. Hence there exists a critical voltage that must be overcome for continuous formation of columnar flow. Beyond the critical voltage, the plots for flow rate are approximately correlated by a straight line. Bologna et al. (2007) have examined the EHD flows of purified transformer oil in a multielectrode system and shown the similar tendency, that is, the existence of critical value and relationship by a straight line for voltage dependence of flow velocity. The acceleration of increase in height at high voltages can be easily expected from Fig. 3.

In EHD pumps and inkjet devices, the electric energy is directly converted into kinetic energy of the fluid. To establish the methods of controlling the flow and optimizing the operating conditions, it is important to evaluate the performance of devices in terms of energy conversion. The conversion efficiency is defined as the ratio of kinetic energy of fluids to the electric energy introduced into the system. The former is given by the product of induced pressure and flow rate, and the latter by the product of applied voltage and current. Figure 6 shows the energy conversion efficiency plotted against the applied voltage. Since the water column from the nozzle tip disappears at voltages below 4.0 kV, the values cannot be determined. The energy conversion efficiency begins to rapidly increase above critical

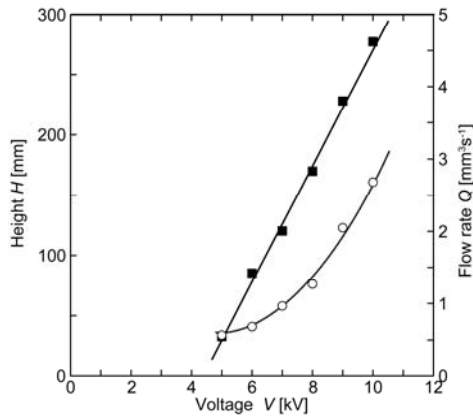


**Fig. 5. Height of water column(○) and flow rate(■) plotted against the applied voltage for ion-exchanged water.**

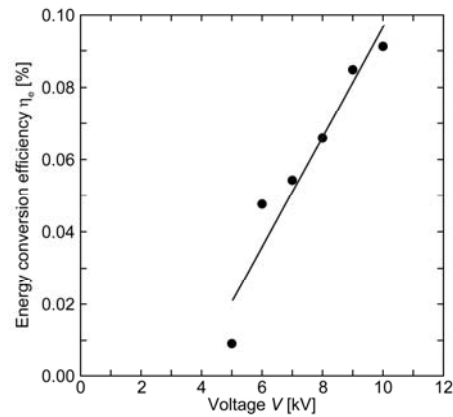


**Fig. 6. Energy conversion efficiency plotted against the applied voltage.**

voltages and seems to reach the saturation at high voltages. The attained efficiency is estimated to be about 0.1% at voltages above 10 kV. The high values of pressure induced in electric fields and energy conversion efficiency is attractive in the practical application of EHD technology.

### 3. EHD MOTORS AND THE EFFECTS OF FLUID PROPERTIES

To convert the electrically induced force to macroscopic flow in the liquid, a prototype of motor, which is shown as a schematic picture in Fig. 7, is designed. The motor consists of wheel with eight vanes, cup, two sets of electrodes, and working fluid. The vane wheel and cup are made of polystyrene, and the electrodes are platinum needles with a diameter of 0.20 mm. The lengths of positive and negative electrodes which are exposed to working fluid are 3.0 mm and 1.0 mm, respectively, and they are arranged at a sector angle of 45°. Two sets of electrodes are symmetrically placed around the inner wall of cup. The working fluid is filled to completely immerse the vanes.

On the application of a high DC voltage to the positive electrodes, the vane wheel begins to rotate counterclockwise at a constant speed. Figure 8 shows the relation between the angular velocity and applied voltage. The working fluid is distilled water. The velocity slowly increases at low voltages and above 2.0 kV rapidly increases with increasing the voltage. At 7.0 kV the rotation speed is about 300 rpm and this value is acceptable in practical use. The current at 7.0kV is 1.2 mA for one set of electrodes and the energy consumption of motor is about 17 W. The jet flow from the negative electrodes is effectively converted to circulation flow along the cylinder wall which contributes to the rotation of vanes. Supposed

that the EHD flow generated from the electrodes along the inner wall of cylinder has the same angular velocity as the rotation of vane wheel, the velocity of

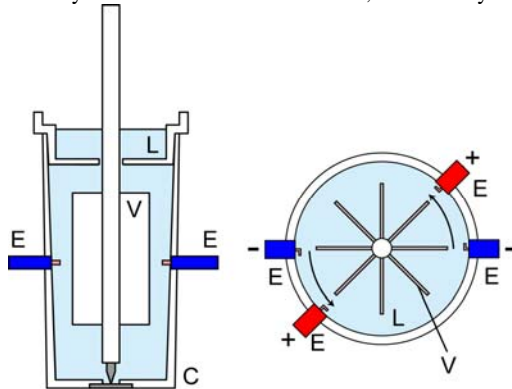


**Fig. 7. A schematic picture of liquid motor: (C) cup, (E) electrodes, (L) working fluid, and (V) vane.**

jet is estimated to be  $0.3 \text{ ms}^{-1}$ . One can easily understand that the fundamental concept shown in Fig. 7 is very attractive as a new type of liquid motors, which utilize an EHD jet of water.

Next interest is the relation between motor performance and fluid properties. To examine the effects of fluid properties, aqueous solutions of ethanol and glycerin were used as working fluids. The viscosity and conductivity at  $25^\circ\text{C}$  are shown in Table 1. The viscosity was measured by the use of oscillating plate viscometer (SV-10 manufactured by A&D Co. Ltd.,). In this instrument, the viscosity is determined by detecting the driving electric current necessary to resonate the two sensor plates at constant frequency of 30 Hz. The conductivity was measured at different field strengths under the condition of several  $\text{mA}\cdot\text{m}^{-2}$ . The motor shown in Fig. 7 was filled with working fluids and the angular velocity was measured at different voltages.

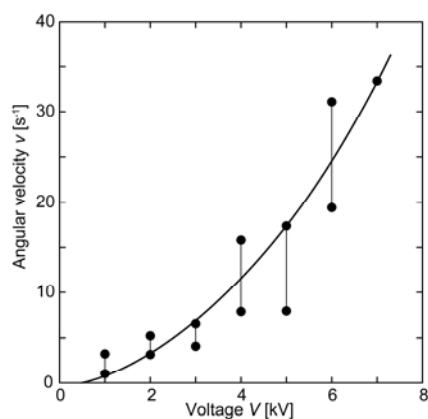


**Fig. 8. Angular velocity of motor plotted against the applied voltage for ion-exchanged water.**

Figure 9 shows the results for aqueous solutions of glycerin. For solutions at glycerin concentrations to 75 wt%, the steady rotation is achieved above some critical voltages. The angular velocity at a fixed voltage decreases with increasing the glycerin concentration. However, the concentrated solutions beyond 75 wt% do not act as working fluids even at 7.0 kV. At the beginning of electrification, the instantaneous motion of vane wheel occurs in the narrow regions, but the motion rapidly declines in a few seconds. Although the circulation flow of fluids is generated near the electrodes, it does not contribute to the continuous rotation of vane wheel.

Figure 10 shows the angular velocity plotted against the applied voltage for aqueous solutions of ethanol. In a similar manner to glycerin, the addition of ethanol causes the reduction of motor speed. But the angular velocity is not given by a monotonously decreasing

function of concentration. It looks likely that the EHD

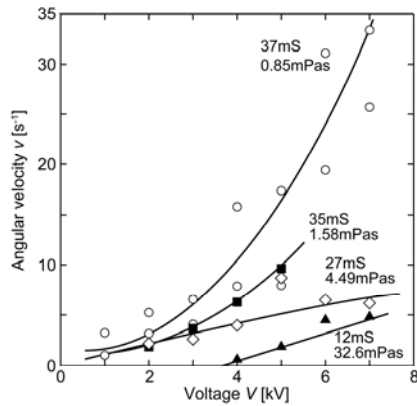


**Fig. 9. Angular velocity of motor plotted against the applied voltage for aqueous solutions of glycerin at different concentrations: 0(○), 25(■), 50(◇), 75wt% (▲).**

**Table 1 Viscosity and conductivity of solutions**

Mixing ratio of solutions			Viscosity $\eta$ (mPa·s)	Conductivity $\sigma$ (mS $\cdot$ m $^{-1}$ )
Water (wt%)	Ethanol (wt%)	Glycerin (wt%)		
100	-	-	0.85	37
75	25	-	1.38	32
50	50	-	2.22	30
25	75	-	1.68	20
-	100	-	0.97	3.7
75	-	25	1.58	35
50	-	50	4.49	27
25	-	75	32.6	12
-	-	100	641	0.61

ability to convert the electric energy to kinetic energy shows a minimum at 50 wt%.

decreases with increasing concentration. The fluids

According to previous work in which the EHD behavior has been examined for twenty-three kinds of insulating oils (Otsubo and Edamura 1999), the factors controlling the motor performance are viscosity and conductivity of solutions. For glycerin solutions, the viscosity increases and conductivity

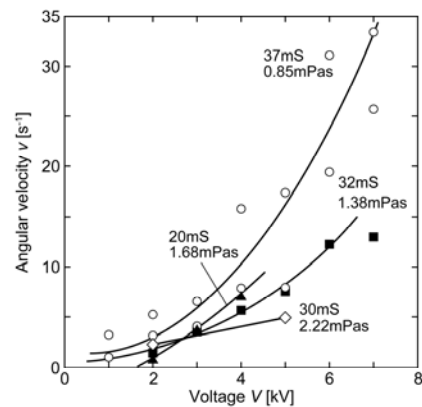


**Fig. 10. Angular velocity of motor plotted against the applied voltage for aqueous solutions of ethanol at different concentrations: 0(○), 25(■), 50(◇), 75wt%(▲).**

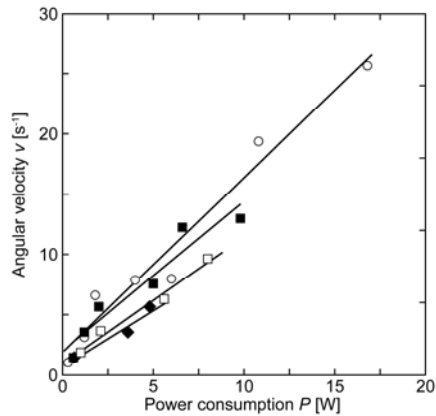


**Fig. 11. Angular velocity plotted against the power consumption: distilled water (○), 25% aqueous solutions of ethanol (■), 75wt%, aqueous solutions of ethanol (□) and 25% aqueous solutions of glycerin (◆).**

with low viscosity and high conductivity can provide high performance of EHD motors. The viscosity of ethanol solutions increases passes through a maximum and then decreases with increasing concentration. Good correlation can be seen between the motor speed and viscosity, except for pure ethanol. It is considered that for pure ethanol the low viscosity does not effectively contribute to high speed of motor, because of low conductivity. Combining Fig. 9 and 10, the high performance of motor is achieved by the solutions with viscosity of 0.85~1.7 mPa·s and conductivity of 20~30  $\mu\text{Sm}^{-1}$ . For motors employing these solutions as working fluids, the angular velocity is shown in Fig. 11 as a function of power consumption that is given by the product of applied voltage and current. The plots for each solution approximately lie on a straight line. This behavior can be related to the quadratic dependence of column height on the voltage in inkjet device. Therefore, the forces induced in EHD process of water and water-based solutions may be proportional the square of field strength.

#### 4. CONCLUSIONS

On the application of high DC electric fields to distilled water through needle electrodes, the jet flow with velocities up to 0.3  $\text{ms}^{-1}$  is generated in bulk from the negative to positive electrodes. By modification of the electrode shapes and geometrical

arrangements, new types of inkjet devices and liquid motor are developed. For aqueous solutions of ethanol and glycerin, the angular velocity of motor is measured as a function of viscosity and conductivity. The high performance of motor is achieved by the solutions with viscosity of 0.85~1.7 mPa·s and conductivity of 20~30  $\mu\text{Sm}^{-1}$ . The EHD water jets have great potential in development of new fluid devices.

#### ACKNOWLEDGEMENTS

This work was supported by a Grant-in-Aid for Scientific Research from the Ministry of Education, Culture, Sports, Science and Technology, Japan, for which the authors are grateful.

#### REFERENCES

- Bologa, M.K., Grosu, F.P., and Kozhevnikov, I.V. (2007). Features of electrohydrodynamic flows in a multielectrode system, *Surf. Eng. Appl. Electrochem.* 43, 434-438.
- Bologa, M.K. and Kozhevnikov, I.V. (2008). Electrohydrodynamic pump characteristics at different parameters of the interelectrode space, *Surf. Eng. Appl. Electrochem.* 44, 285-287.
- Castellanos, A. (1991). Coulomb-driven convection in electrohydrodynamics. *IEEE Trans. Electr. Insul.* 26, 1201-1215.
- Darabi, J., Rada, M., Ohadi, M.M., and Lawler, J. (2002). Design, fabrication, and testing of an electrohydrodynamic ion-drag micropump, *J. Microelectromech. Syst.* 11, 684-690.
- Darabi, J., Ohadi, M.M., and DeVoe, D. (2001). An electrohydrodynamic polarization micropump for electronic cooling, *J. Microelectromech. Syst.* 10, 98-106.
- Darabi, J. and Wang, H. (2005). Development of an electrohydrodynamic injection micropump and its potential application in pumping fluids in cryogenic cooling systems, *J. Microelectromech. Syst.* 14, 747-755.
- Darabi, J. and Rhodes, C. (2006). CFD modeling of an ion-drag pump, *Sens. Actuators A* 127, 94-103.
- Edamura, K. and Otsubo, Y. (2004). A continuous inkjet device on the basis of electrohydrodynamic mechanism. *J. Imaging Sci. Technol.* 48, 148-152.
- Gosse, J.P. (1988). Electric conduction in dielectric liquids. *NATO ASI Ser B* 193, 503-517.

- Haga, M., Maekawa, T., Kuwahara, K., Ohara, A., Kawasaki, K., Harada, T., Yoda, S., and Nakamura, T. (1995). Effect of electric field on Marangoni convection under microgravity. *J. Jpn. Soc. Microgravity Appl.* 12, 19-26.
- Maekawa, T., Abe, K., and Tanasawa, I. (1992). Onset of natural convection under an electric field. *Int. J. Heat Mass Transfer* 35, 613-621.
- Otsubo, Y. and Edamura, K. (1997). Dielectric fluid motors. *Appl. Phys. Lett.* 71, 318-320.
- Otsubo, Y. and Edamura, K. (1998). Viscoelasticity of a dielectric fluid in nonuniform electric fields generated by electrodes with flocked fabrics. *Rheol. Acta* 37, 500-507.
- Otsubo, Y. and Edamura, K. (1999). Electric effect on the rheology of insulating oils in electrodes with flocked fabrics. *Rheol. Acta* 38, 137-144.
- Park, C.H., Kim, K.H. Lee, J.C., and Lee, J. (2008). In-situ nanofabrication via electrohydrodynamic jetting of countercharged nozzles. *Polymer Bull.* 61, 521-528.
- Rocks, S.A., Wang, D., Sun, D., Jayasinghe, S.N., Edirisinghe, M.J., and Dorey, R.A. (2007). Direct writing of lead zirconate titanate piezoelectric structures by electrohydrodynamic atomization. *J. Electroceram.* 19, 287-293.
- Skotak, M. and Larsen, G. (2006). Solution chemistry control to make well defined submicron continuous fibres by electrospinning: the (CH<sub>3</sub>CH<sub>2</sub>CH<sub>2</sub>O)<sub>4</sub>Ti/AcOH/poly(N-vinylpyrrolidone) system. *J. Mater. Chem.* 16, 3031-3039.
- Suzuki, M. (1985). Propagating transition of electroconvection. *Phys. Rev. A* 31, 2548-2555.
- Wang, D.Z., Jayasinghe, S.N., Edirisinghe, M.J., and Luklinska, Z.B. (2007). Coaxial electrohydrodynamic direct writing of nanosuspensions. *J. Nanoparticle Res.* 9, 825-831.
- Worraker, W.J. and Richardson, A.T. (1981). A nonlinear electrohydrodynamic stability analysis of a thermally stabilized plane layer of dielectric liquids. *J. Fluid Mech.* 109, 217-237.
- Yasufuku, S., Umemura, T., and Tanii, T. (1979). Electric conduction phenomena and carrier mobility behavior in dielectric fluids. *IEEE Trans. Electr. Insul. EI* 14, 28-35.
- Yokota, S., Hirata, M., Kondoh, Y., Suzumori, K., Sadamoto, A., Otsubo, Y., and Edamura, K. (2001a). Micromotor Using Electroconjugate Fluid(Fabrication of Inner Diameter 2 mm RE Type ECF Motor). *J. Robotics Mechatronics* 13, 140-145.
- Yokota, S., Sadamoto, A., Kondoh, Y., Otsubo, Y., and Edamura, K. (2001b). A Micromotor Using Electroconjugate Fluid(ECFs) (Proposition of Stator Electrode Type(SE-type) micro ECF Motors). *JSME International J. C* 44, 756-762.
- Zahn, J.D. and Reddy, V. (2006). Two phase micromixing and analysis using electrohydrodynamic instabilities. *Microfluid Nanofluid* 2, 399-415.